International Journal of Recent Technology and Engineering (IJRTE)
ISSN: 2277-3878, Volume-8 Issue-3, September 2019

An Effective Detection Method of Glioma Tissue in Multimodal Brain Image using Adaptive Segmentation Algorithm

Perumal.B, Sindhiya Devi.R, Pallikonda Rajasekaran.M

Abstract*: In the medical field, accurate and faster classification and segmentation of tumor images in the brain is enormously crucial. In our paper, we introduce a distinct process to segment the multimodal brain image and to find out the tissues affected by glioma. Skull stripping is the preprocessing method to remove non-cerebral tissues. Later, the image is segmented using an Adaptive segmentation Algorithm (ASA) process, after doing primary segmentation to find out the consistent regions for the process of integrating images. It reduces over segmentation and conserves the frontiers of the image. The adaptive segmentation process follows the four steps: exemplification of the region and similarity measure, marking of the object and background, merging rule based on maximal homogeneity and the process of unifying. The segmented output image can clearly view the region that selected. From the image segmentation, several features are extracted including mean, variance, entropy using Gaussian Inception (GI) method. After feature extraction, classification is done using Support Vector Machine (SVM) classifier which classifies the voxels into normal and affected one. This proposed method could be used in the easier and effective diagnosis of brain tumour in brain MRI images. The diagnosis of brain tumour by using this interactive adaptive segmentation will be more accurate as in human investigation and at the same time classification is done at a faster rate as in fully computerized investigation. The method is evaluated experimentally using multimodal brain images of patients with glioma. The classification results of the proposed methodology are compared with the existing method which shows the improved accuracy.

Keywords: Glioma, Merging process, SVM classification, Gaussian Inception.

I. INTRODUCTION

Gliomas are one kind of brain tumors, which is seemed habitually. Glial cells presenting in the brain cause gliomas. This tumor develops by permeating the contiguous tissue. The more destructive kind of glioma is considered as high-grade glioma.

Manuscript published on 30 September 2019
***** Correspondence Author
B.Perumal*, Associate Professor/ECE, Kalasalingam Academy of Research and Education, Srivilliputhur, India. Email: palanimet@gmail.com
R.Sindhiya Devi*, Research Scholar/ECE, Kalasalingam Academy of Research and Education, Srivilliputhur, India. Email: sindhiyadevi14@gmail.com
Pallikonda Rajasekaran, Professor/ECE, Kalasalingam Academy of Research and Education, Srivilliputhur, India. Email: mpraja@klu.ac.in

The tumor develops rapidly and the lifetime of the patients will become very low about less than two years.
Therefore, the treatment must be offered as soon as the disease is diagnosed. Another kind of glioma that matures gradually is known as low-grade glioma and the lifetime of the patients with this low-grade glioma is generally five years [1]. Numerous neuro imaging algorithms are employed during treatment to get the images of tissue with a view to appraise the tumor condition and the victory of a given treatment. In order to perform the assessments frequently, the enormous amount of multimodal longitudinal datasets is created for these patients.
The multimodal medical images are obtained by incorporating several techniques that includes Nuclear Medicine Technique, Positron Emission Tomography Imaging, Magnetic Resonance Imaging and Optical Imaging. The imaging technique for the multimodal images plays a vital role in various fields of medicine for imaging. It exhibits enormous applications in many areas from molecular pharmacology to nanotechnology field [2]. One kind of multimodal image is obtained from the combination of usage of Positron Emission Tomography-Single-Photon Emission Computed Tomography (PET-SPECT) and Positron Emission Tomography-Computed Tomography (PET-CT) scanner techniques. This kind of combination of multimodality is used extensively. Another type of multimodal image is the integration of 2-D Electro Encephalography (EEG) and Magneto Encephalography (MEG) methods. The combination of EEG/MEG is due to the straight connection of the detected signals to neuronal electrical function. That is, EEG and MEG expose the electric and magnetic fields created by synaptic trans-membrane currents happened in neurons. In MRI scans, the different MRI measures are functionally registered among them. At first the registration process was accomplished between T2-W MRI and the X-ray by taking MRI as reference and X-ray as the input through normalized mutual data. In another kind, the PET measures were registered to the MRI factors. ROIs outlined on T2-W MRI images were relocated onto the PET images.
Glioma is a rapidly developing tumor having disseminated margins and lesion regions. It is delineated through the variations of intensity depending on the contiguous ordinary tissues. However, the marked regions of tumor by manual segmentation are often inconsistent.

The methods used for normalizing MR intensity are unsuccessful if the image contains extended lesions. In general, tumors vary substantially in its dimension, outline, and position. The inflation which is appeared because of the enlargement of the tissues may drift the normal tissues of the brain.

In addition, a resection cavity produced due to the treatment restrains the consistency of former data accessible for the normal portions of the brain tissue. In order to represent these changes, many imaging modalities are presented and from these modalities, various data regarding brain tissue are obtained. The obtained data are

- Alterations in tissue water
- Augmentation of contrast agents
- Water diffusion
- Blood perfusion
- Comparative absorptions of certain metabolites

Brain tumor segmentation process for glioma takes place in many research works. Some techniques have been proposed earlier, which can be utilized for mild tumors occurring occasionally. Brain lesions are produced by traumatic brain injuries [3], [4] and stroke [5], [6]. These lesions look like glioma lesions relative to the dimensions and multimodal intensity forms. The segmentation processes utilized to segment brain lesion are generally based on either proliferous type or excludent for their processing stage. These segmentation algorithms determine former details regarding spatial regularity and tumor configurations. Several algorithms provide longitudinal dimensions for 4D images to utilize longitudinal images.

In this paper, the proposed segmentation is obtained from Interactive process. This method primarily segments and merges the homogenic portion of the affected tissues from the normal tissues. Besides, the proposed method brings about standardization of the patient tumor from the growth model measures. The standardization of the image is important to provide treatment and to discover the patient's lifetime. The measurement of extra factors makes the process complex. The proposed segmentation yields accurate information of the tumor dispersal. Section 2 and section 3 discusses about the various segmentation algorithms along with the proposed methodology presented for gliomas, respectively. Section 4 talks about the observed results and section 5 provides with the conclusion.

II. LITERATURE SURVEY

In work [7], FCM clustering is introduced to the MRI data sets of a glioma tumor. By using fuzzy segmentation, they obtained tumor volume of the patient in 3 dimensions. The tissue margins were represented using gross and histopathological correlation. Similarly, in the work [8], knowledge based methods were presented to construct more sophisticated attributes from multi-modality MR images for FCM. In an alternative work [9], a novel method is suggested to extract the 3D associated constituents of the segmented tumor voxels. Thus, this method was utilized to remove the false positives (FP). However, this method did not work effectively for more amounts of data sets due to the requirement of the improved sophisticated process. The spatial smoothness varied in relation to the curvature smoothing feature which provided less curve outflow in the background. Another kind of segmentation process depends on the pattern classification methods. These methods are of two major types known as discriminative and generative approaches. Generative methods unambiguously characterize a pattern for the voxel distribution of labels and variables. In contrast, excludent methods produce a system which realizes the voxels trained on their intensities.

The work [10] presented pseudo-conditional random fields. It is a normalized discriminative classifier and classifies the voxels based on the labels and aspects of adjacent voxels. The spatial interface of the adjacent voxels is unswervingly arranged on the successive probabilities, with the use of a potential function obtained from voxel labels and intensities. Generally, highly complicated, voxel – wise attributes are given as input to deep learning methods.

On the work [11], registration of data collection based on probability that has even space is performed to fix the former probabilities of normal tissues. Then a set of data for training to identify normal tissue voxel attributes was developed. In [12], the probabilistic boosting trees were employed [13] to realize the likelihood predictions from the data set for training. Also it employs Markov Random Field algorithm as the preceding expectation of the tissues. In [14], likelihoods were calculated by means of a Gaussian Mixture Models and a graph structure. The benefit of generative methods compared to the discriminative methods is that they offer an organized structure to unambiguously design the spatial smoothness by means of previous probabilities of the labels. In Maximum A Posteriori (MAP) estimation method, the latter probability of all labels were estimated using the Bayes rule and maximized. There are many other methods to obtain maximization are graph cut methods [12], that includes Expectation - Maximization algorithm [14], and level set methodology [11].

As for denoising the MRI images, several techniques have been implemented where some of them are Non-Local Means (NLM) [19-21], Wavelet Transform (WT) [17, 18], Independent Component Analysis (ICA) [22, 23] and Anisotropic Diffusion Filtering (ADF) [15, 16]. Among these methods, ADF is a popular technique to de-noise the MRI images figuring brain tumor. In [24], the common problems which result with several effects due to noise reduction methodologies on brain tumor images for segmentation were conferred. However, this work [24] inferred that there is presence of noise on the tumor image after segmentation shows the negativity in the result, though the image noise was reduced. These drawbacks are overcome by skull stripping method which is said to be an intrinsic step of preprocessing in the analysis of MRI images [25-28]. The delimitation process is defined by the elimination of some of the non-cerebral hard tissue regions including scalp and the skull from the soft tissues of the brain [29]. In another work [30], it described that skull stripping method is influenced in determining the tumor presence along with the brain morphometric after pre – planning and the reconciliation of the cortical surface [30],

whereas another work [31] implies that it is very essential for the splitting up of brain tumor. It is obvious that elimination of the skull limits the misclassification in tumor affected tissues [32].

The skull stripping technique is confronted with a lot of dares all because of the entanglement in the human brain and some other distinct factors along with the variable parameters of MR monitors [33]. Besides, mediocrity and low disparateness of images leads to struggle in the precise image segmentation [32]. These drawbacks can be overcome by several approaches [34]. However, intensity normalization [35] is required for the MRI preprocessing, when segmentation process handle classification and clustering methods. Because of the perplexing effects caused by the variances in this tumefaction, the splitting out of tumor-hauling images are more formidable rather than healthy images. A patho - biological based highly powerful normalization method for the MR images was proposed so as to embelish the constraints both global and local [36]. Actually, in order to restrict the magnetic field effect, a bias-field correction was used in homogeneities during image acquisition [37]. In most cases, a rectilinear model for transformation with the Mutual Information (MI) homogeneity criterion is used [38] to guarantee voxel to voxel communication throughout the different modalities.

III. PROPOSED METHODOLOGY

In this paper, multimodal high dimensional brain image obtained from MRI is processed as in figure 1. Initially we use a planetary threshold value to transfer the intensity image as the binary image. The global threshold value is a standardized intensity value, which is in the range [0, 1]. The dispersion of intensities in the gray scale image is denoted by means of the histogram. The preprocessing used here is the skull stripping method. Then generative segmentation model based on Adaptive Segmentation (ASA) Algorithm is done. With the intention of extracting features from the multimodal image, Gaussian Inception (GI) is employed. Then the voxel labels are classified using Support Vector Machine (SVM) classifier.

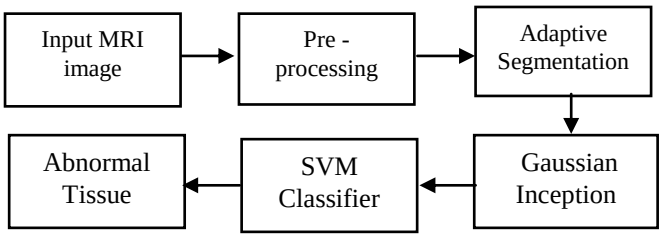

Fig. 1.Block diagram of proposed method

A. *Pre-processing*

In general, MRI preprocessing methods are applied before the segmentation to achieve the better result since preprocessing could straightly change the attributes of the segmentation. We undertake preprocessing the MR images for comprehending the segmentation purposes. In pre-processing, MRI images undergo several proceedings that include noise removal, skull eviction as well as the regularization of its intensity. Generally, most of the researchers use noise filtering in the image as a customary process. MRI image usually affected by noise and hard to distinguish the regions belonging to the tumefacted tissues from the normal tissues of brain. Therefore, it is clear that preprocessing is necessary in case of MRI images for the reduction of noise and enhancement of the contrast between the regions.

Skull stripping is the process of isolating the soft tissues of the brain from the harder cranial bones. This process should be authentic and convincing; otherwise we may obtain the erroneous judgment about the brain images. Recent technologies depend on fact – based geometric notions even when the image is not perfectly registered and not visualized flawlessly for its features. In our work, we use thresholding by the method of Otsu in order to determine the image threshold and apply labels correspondingly. The assumption that the histogram intensity has to be bi – modal is being done in this thresholding. Later, buffing of images is done with the help of Gaussian averaging filter. It helps in providing an easily distinguishable forefront and backdrop. This is done by manipulating the variance between images of different classes and reducing the usage of variance between images of same class.

However, we alter the image from monochrome into a double – barreled image. The arithmetical clarification of Otsu's method is defined by the expression given below:

$$\sigma_w^2(t) = w_0(t)\sigma_0^2(t) + w_1(t)\sigma_1^2(t) \quad (1)$$

Here, $\sigma_w^2(t)$ is the intra-class variance. It is estimated by the summation of the weighted variance of the two distinct classes. The individual weights are estimated as follows:

$$w_0(t) = \sum_{i=0}^{t-1} p(i) \quad (2)$$

$$w_1(t) = \sum_{i=t}^{L-1} p(i) \quad (3)$$

Here, p(i) is the intensity Adaptive of the individual pixels. Otsu's method also shows that minimizing the intra-class variance also capitalizes on the inter-class variance as:

$$\sigma_b^2(t) = \sigma^2 - \sigma_w^2(t) \quad (4)$$

$$\sigma_b^2(t) = w_0(\mu_0 - \mu_T)^2 + w_1(\mu_1 - \mu_T)^2 \quad (5)$$

$$\sigma_b^2(t) = w_0(t)w_1(t)[\mu_0(t) - \mu_T(t)]^2 \quad (6)$$

B. *Adaptive Segmentation Algorithm (ASA)*

In this routine, we are in need of a segmentation to be done initially so as to find out the consistent regions for the process of integrating images. There are several primary stage segmentation methods used for this purpose where some of them are super-pixel [39], mean shift [40, 41], watershed [42] and level set [43]. In this analysis, the mean shift algorithm is preferred since there exist only smaller amount of over segmentation and the frontiers of the specific image portion could be conserved.

Steps Involved:

Step 1: Exemplification of Domain and Similarity Measure

The leadoff partition is done by mean shift method. After this, we find a large amount of miniature portions to be present. These minute portions should be exemplified by means of some descriptor and a principle should be formalized in order to lead the way for merging.

We can express a region in different ways that include appearance, composition and margin [44] of the region. Here, we have applied binary image for the segmentation process. Each channel in each region is quantized at a uniform rate as such into 16 levels and then their histogram is estimated in the feature space of 16×16×16=4096 bins. For region A, the standardized histogram is represented by HA. Next, we have to know the way to combine the regions in conformity with their intensity so that we could extract the desired object. Here, we distinguish the glioma as the main object and the rest of the brain as background regions. In region merging, we are in need to find the way to get the homogeneity between unblotted and the blotted regions. It is done so in order that we could combine the matching portions together with some analytical reason. We should describe a measure of homogeneity among the regions A and B as ρ (A, B) in order to bring about the distinction between different portions. There exists a lot of prominent and notorious metrics that are pertaining to statistics like Euclidean distance, Bhattacharyya coefficient and the log-likelihood ratio statistic [48]. Here the Bhattacharya coefficient (ρ) has been chosen in order to find out the homogeneity measure between A and B

$$\rho(A,B) = \sum_{i=1}^{4096} \sqrt{H_A^i H_B^i} \quad (7)$$

where H_A^u is the standardized histogram of A and H_B^u is the standardized histogram B. Their ith element is expressed by the superscript i. Bhattacharyya coefficient is a standard that interprets in a direct way of geometrical deviance. It is defined by taking the unit vectors' cosine angles.

$$\left(\sqrt{H_A^1}, \ldots, \sqrt{H_A^{4096}}\right)^T \text{ and } \left(\sqrt{H_B^1}, \ldots, \sqrt{H_B^{4096}}\right)^T \quad (8)$$

If the value of the Bhattacharyya coefficient between A and B is in greater number, then the homogeneity relation between them is also in greater number. The Bhattacharyya coefficient always betrays that the regions are perceptually similar. The Bhattacharya coefficient depends mainly on the contents of the two regions, so that the similarity in the two regions causes their histograms to be similar which automatically increases the value of Bhattacharya coefficient. It is nothing but it decreases the angle between the histogram vectors. There is a certain possibility of geometrically distinct portions to have homogeneity in their histograms. But these cases are not common because the histograms in these regions are local which reflect the local attributes of the images. Even if the two geometrically distinct portions with similar histograms arise, the highest homogeneity with the neighborhood is uncommon. Coupling with the "maximal similarity rule", the Bhattacharyya similarity harmonizes with the recommended region merging method. Rather than its simplicity, the descriptor of Bhattacharyya method is paves an efficient way for region exemplification and homogeneity measurement. This method has been used in a victorious way to find out the resemblance between the target model and candidate model in the object tracking method which is based on its kernels [47].

Step 2: Characterization of Entity and Backdrop

The next step in the interactive image segmentation is to mark the main object and the backdrop notionally. We can get the input data which is informative from the drawing markers such as lines and strokes as in [49-51]. The glioma tissue regions can be considered as the object marker regions, while the rest of the brain region is considered as the background marker region. If we need reduced number of required inputs, then the interactive algorithm tends to be more appropriate and powerful. Once when the object marking is done, labeling of every portion of the image is done as either one of the different regions which are the blotted entity, the blotted backdrop and the non-blotted region. Now we should assign each non-blotted region as either entity or backdrop region in order to obtain the object. The blotted entity regions and the blotted backdrop regions are represented by MO and MB respectively, whereas the unblotted regions are denoted as X.

Step 3: Homogeneity Based Merging Rule

After characterization of entity and backdrop, we have still a lofty goal to deduce the entity from the backdrop in greater accuracy as there exist only a minuscular portion of the entity/backdrop attributes are represented initially. With the object and the background markers, we could find out all the unblotted portions based on the maximal homogeneity. Let B be the nearby portion of A and is indicated by i=1,2,...,b.

In MSRM, only color information is used to judge the similarity. The homogeneity between B and all its adjoining regions i.e. $\overline{S_B} = \{S_i^B\}_{i=1,2,\ldots,q}$ are then estimated. It is so obvious that A is a member of $\overline{S_B}$. The integration of A and B will be done only if the homogeneity between A and B is the ultimate among all the homogeneities ρ (B, S_i^B). The integrating rule is expressed as follows:

Merge A and B if $\rho(A,B) = \max_{i=1,2,3,\ldots,b} \rho(B, S_i^B)$ (9)

Here, "max" operator avoids a preset similarity threshold, however somewhat sensitive to noise. It has the following limitations: 1) Fails when low contrast edges occurs.

2) Fails when part of the object region is slightly more similar in color to some background regions or vice versa.

To solve this problem, we present an adaptive maximal similarity based merging (mMSRM) mechanism. It takes into account both the color similarity and the spatial distance of the candidate regions for merging. For two regions A and B, we define the spatial distance as

$$\rho_s(A,B) = \|\text{center}_A - \text{center}_B\|_2 \quad (10)$$

where, center_A and center_B – center pixels of region A and B

$\|.\|_2$ - Euclidean distance

The lower the spatial distance, the higher is the spatial similarity between them. Directly integrating spatial distance into the color similarity computation, we define

$$\rho(A,B) = \exp\left(-\frac{\rho_s(A,B)}{\sigma^2}\right).\rho_c(A,B) \quad (11)$$

Step 4: Unifying Process

Rather than its simplicity, the merging rule (9) that is stated above shows the recommended region merging process' basic properties. It has its significance of avoiding the pre – arrangement of threshold in its homogeneity in order to control the merging process. Here, the "max" attribute changes according to the aberrations and it harmonizes with our algorithm. This is because the histogram is reactive even to small variability as it is a globular inscription of the confined region.

The Bhattacharyya coefficient is also sensitive to the miniscular differences as it is the intramural artifacts of the two histogram trajectories. The object and the background have only a limited portion as marker zones. Those non – marker object regions which are the unblotted entities has to be ascertained rather not be amalgamated amidst the backdrop. The unblotted object regions are from the same object and so it possesses greater homogeneity with the blotted object portions in contrast to the backdrop locale. Hence, in the self – executing zonal unification process, the unblotted object regions recognizes them as object with elevated plausibility.

We can analyze the contingency of the tumor presence in the path of voxel i by casting up all the setouts Mo after reckoning the model parameters $\rho(A, B)$.

$$p(M_o{}^c|y;\ \rho) = \sum_{M_o} M_o{}^c p(M_o|y;\rho) = \sum_{M_o} M_o{}^c x_i(M_o) \quad (10)$$

where c- channel and x_i – posterior probability. Then, the channel c of voxel I should be allocated to tumor if $p(M_o|y;\rho)$>0.5.

C. *Feature Extraction*

In this paper, Gaussian Inception (GI) is a novel technique applied for the extraction of features in which the difference of offset Gaussian model with specific threshold is employed over the image. The implementation of GI for feature extraction process helps to obtain extensive details of the feature value with respect to time and frequency domain which helps for image classification. From the GI model, the obtained feature values are applied to the classifier using feature selection process. In case of GI model, the value of σ is altered over a wide range which provides many features according to time and frequency domain. By implementing a large number of GI models, numerous features can be obtained and the ideal features will be nominated among them. In this technique, the loss of significant data is greatly reduced and the classification process has sufficient data for further processing. The Gaussian Distribution (GD) function of a given image is obtained from the Equation (13). The first derivative of this image is obtained by Equation (14). However, when the input image has noise, the first derivative of the Gaussian provides noisy image. This noise can be eradicated by estimating Difference of Gaussian (DoG) which is derivative (GD). For the proposed application of detecting the feature value, the GD provides better features than DoG provides. Hence Gaussian Inception (GI) can be arrived at the better solution since it is the primitive Gaussian with the noise removal factor. Thereby, we place the Gaussian signal at an offset distance d and the thresholded difference between these two signals is calculated as in Equation (15).

$$G_\sigma(x) = \left(\frac{1}{\sigma\sqrt{2\pi}}\right) e^{\frac{-(x^2)}{2\sigma^2}} \quad (13)$$

$$GD_\sigma(x) = \frac{\partial G_\sigma(x)}{\partial t} = -\frac{x}{\sigma^3\sqrt{2\pi}} e^{\frac{-(x^2)}{2\sigma^2}} \quad (14)$$

$$GI_\sigma(x) = \begin{cases} G_\sigma(x) if\ G_\sigma(x) > G_\sigma(x+d) \\ G_\sigma(x) - G_\sigma(x+d) if\ G_\sigma(x) < G_\sigma(x+d) \end{cases} \quad (15)$$

From the GI signals the standard statistical measures are extracted as given below. The GI signal is considered as a sampled signal with S number of samples. Then the mean of the image is obtained as in Equation (16)

$$Mean, \overline{GI} = \frac{1}{S}\sum_{k=1}^{S} GI_k \quad (16)$$

The standard deviation of the image is obtained using Equation (17)

$$SD(GI) = \sqrt{\frac{1}{S-1}\sum_{k-1}^{S}(GI_k - GI)} \quad (17)$$

The average instantaneous energy, entropy, skew, kurtosis and contrast are measured using Equations (18), (19), (20), (21) and (22) respectively,

$$Energy\ (GI) = \frac{1}{S}\sum_{k=1}^{S} GI_k^2 \quad (18)$$

$$Entropy\ (GI) = \sum_{s=0}^{k-1} GI_k\,(-ln\ GI_k) \quad (19)$$

$$Skew(GI) = \sum_{s=0}^{k-1}(GI_k - \overline{GI})^3 \quad (20)$$

$$kurtosis\ (GI) = \sum_{s=0}^{k-1}(GI_k - \overline{GI})^4 \quad (21)$$

$$contrast\ (GI) = \sum_k k^2 GI_k \quad (22)$$

Apart from the statistical features, the features like positive peak amplitude which is represented as PP (GI), and negative peak amplitude NP (GI), image width, W (GI) and zero crossings, (ZC (GI)) are acquired from the GI signal. The value of σ in determining the Gaussian distribution takes vital impact. Hence in this work, the different GI signals are acquired by changing the value of σ. For each GI signal, these 7 features are removed by varying σ from 0.1 to 1 with the step increment of 0.1. Thus ten DOGs are obtained and 7 features are obtained for each model and hence it results in 70 (7x10) features. Then all the extracted features are applied to the SVM classifier to categorize the glioma tissue from the normal tissues.

D. *SVM Classifier*

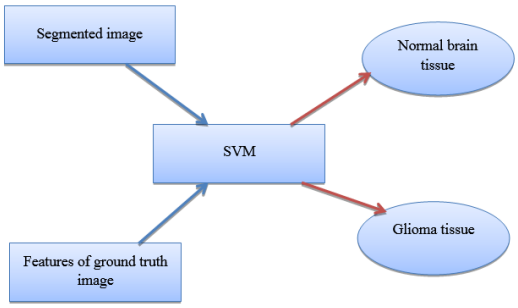

Fig. 2.SVM Classification

After feature extraction, the voxel labels are classified using the Support Vector Machine (SVM) classifier. SVM classifiers are discriminative classifiers created from machine learning. From the training phase, it finds out a separating hyper plane for the points in the feature plot. A set of labeled positive array is used to construct single-class SVM. It is known as positive training samples [52]. Figure 2 represents the block diagram of the SVM classification used in this paper.

The below dataset is considered for an instance. This is used in the training phase.

$$U = \{u_i | i = 1,2,3, \ldots \ldots l\} \quad (23)$$

where ui is the ith observation and l represents the number of observations.

A feature map presents and it maps the training set into a high-dimensional space. This space is known as feature space F. Therefore, the image of a training sample ui in U is represented as ϕ (ui) in feature space. In the feature space, our strategy is to split the data from the origin with the largest margin. Hence, the objective function for the tumor data is expressed as below,

$$\min_{W\epsilon F,\eta\epsilon R^t,b\epsilon R^{\frac{1}{2}}} W^T W + \frac{1}{vl}\sum_i \eta_i - b \qquad (24)$$

W- Ordinary vector of the hyper plane and it represents the decision boundary

b - Threshold of function f. Function f has the value +1 for tumor area and -1 for non-tumor area outside the tumor tissue

ηi - the slack variable.

IV. EXPERIMENTAL RESULTS

The work is implemented in MATLAB software and derived the output. To implement the proposed method, BRATS dataset (2015) is used. This dataset gives 45 interpreted multimodal glioma images. The training dataset contain slow and high grade types with regular T1, Gadolinium-enhanced T1 (T1c), T2 and FLAIR MR Images. We register all images of a patient to the FLAIR volume and a freely available operation of the IS segmentation with bias alteration is utilized. Image intensities of each channel in each volume are scaled linearly to match the histogram of a reference. Images are obtained for patients having acute and sub-acute ischemic stroke. To determine the effectiveness of the segmentation process, the group of four tumor labels is considered for implementation. After segmentation process, SVM classification is applied. The features of the ground truth image is obtained and given in the training phase of the SVM process. The steps of outputs obtained in the overall segmentation process starting from pre-processing are specified in the Table I.

Table- I: Segmentation Output

Process	Set - 1	Set – 2
Inputs	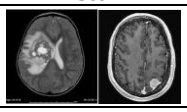	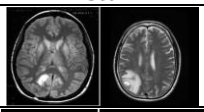
Otsu Method	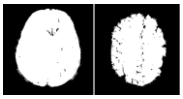	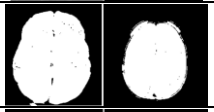
Skull Stripping	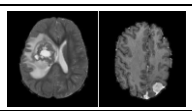	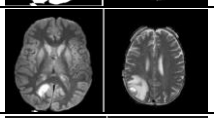
Mean Shift Segmentation	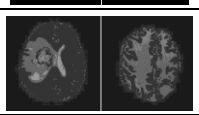	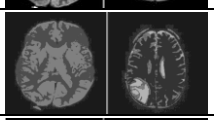
Similarity Measure	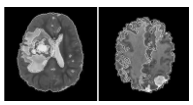	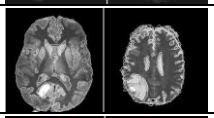
Adaptive Segmentation	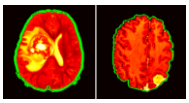	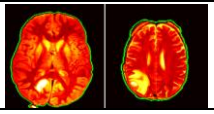

The input MRI image is initially processed under pre-processing method for perfect segmentation. In our work, Skull stripping method is used for preprocessing. Otsu method is used for removing the noise in the MRI image. The result of skull stripping method is free from the noise and skull area.

After preprocessing, the segmentation process follows. In our work, we use the approach Adaptive Segmentation Algorithm (ASA) for segmentation. Before that, mean-shift segmentation is used for low level segmentation. Later, ASA method is done which has four steps for complete segmentation. At first, the similarity of the region is calculated with respect to the level of intensity. The histogram levels of the two adjacent parts are similar. By considering this formula, the similarity measure is done under region representation.

In the next step, the object and the background marking is prepared. In this paper, the glioma affected tissue is considered as the object and the rest of the brain as background marker. After the similarity measure is conducted, we have to mark the object area for the merging process. By doing so, it does not merge with the background which results with better accuracy. The glioma tissues are marked deeply which is the object and the rest as the background.

After the object (glioma tissue) and background (rest of the brain) are completely separated, the merging process has to be done. By considering the maximal similarity in the channel, the image starts to merge iteratively until nothing to merge further. After the completion of merging cycle, the Adaptive segmentation output is achieved as shown in the Table I.

Under the SVM classifier, the output of ASA segmentation is passed to verify whether the given MR image has glioma tissue or normal tissue. From the cells of Adaptive Segmentation in Table I, the tumor and stroke of MR image is classified clearly with the segmentation process. The output image and the ground truth image is send to the classifier and the classifier determines the accuracy.

The accuracy of the work is measured in terms of Average precision, recall, and F -Measure which are defined as

$$F_\beta = \frac{(1+\beta^2)\,Precision \times Recall}{\beta^2 \times Precision + Recall} \qquad (25)$$

$$recall = \frac{True\ positive}{total\ no.of\ positives} \qquad (26)$$

$$precision = \frac{True\ positive}{total\ no.of\ matches} \qquad (27)$$

The performance parameters like accuracy, average mean and classification loss are tabulated in Table II. It figures out that every image has high accuracy with low classification loss. Therefore, the glioma tissue can be easily predicted with accurate result with the combination of Adaptive Segmentation Algorithm (ASA) and Support vector Machine Classifier (SVM).

Table- II: Performance Parameters of the Proposed Work

S. No	Parameters	Input Set 1		Input Set 2	
		Image 1	*Image 2*	*Image 1*	*Image 2*
1	Accuracy	97.23	97.54	98.32	97.96
2	Average Mean	0.45	0.39	0.29	0.35
3	Classification Loss	0.32	0.25	0.31	0.24

The proposed technique is simulated in MATLAB simulation software to evaluate the performance criteria. The MR brain images obtained from different patients in the given dataset are grouped into two types of sets as training sets and testing sets. The distribution is depicted in Table III. 75% of samples are grouped as training dataset and 25% of samples are grouped as testing dataset. In training set, totally 495 samples of glioma are taken and 198 samples are taken for testing. Among the 75% of training samples, around 43.8% of samples are taken from glioma patients, 31.1% are taken from normal patients. Correspondingly, among the 25% of testing samples, around 14.66% are taken from glioma samples and 10.37% data are taken from normal patients.

Table- III: Distribution of Data Set

Group	Glioma samples			Total Glioma samples (%)	Normal samples		Total Normal Samples (%)	Total
	Set-1	*Set-2*	*Set- 3*		*Set- 1*	*Set 2*		
Train set	150	165	180	495 (43.84)	190	200	390 (31.1)	74.94
Test set	60	68	70	198 (14.66)	80	75	155 (10.37)	25.03
Total	200	245	250	695 (58.5)	250	275	525 (23.47)	100

Average mean value, average standard deviation and classification loss of the proposed method are evaluated and tabulated. Total classification loss is reduced by 40% when compared with the existing method [53]. Similarly, the accuracy of the proposed method is 7% higher than the method presented in [53].

The SVM classifier classifies the voxel labels according the features that are extracted. In this paper, the features like mean, standard deviation and energy of the image is considered. The comparison of accuracy and classification loss is depicted in Figure 15 and 16 respectively.

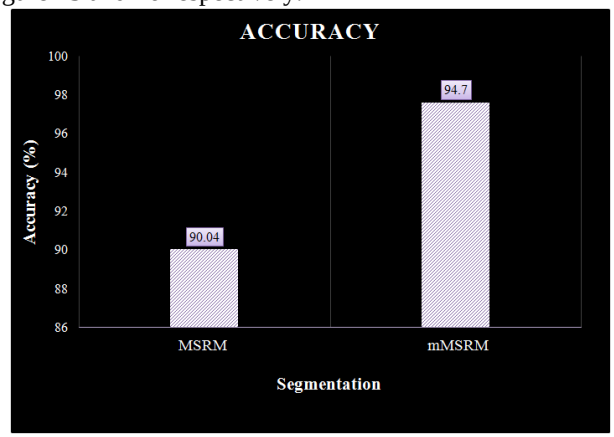

Fig. 3. Accuracy Comparison

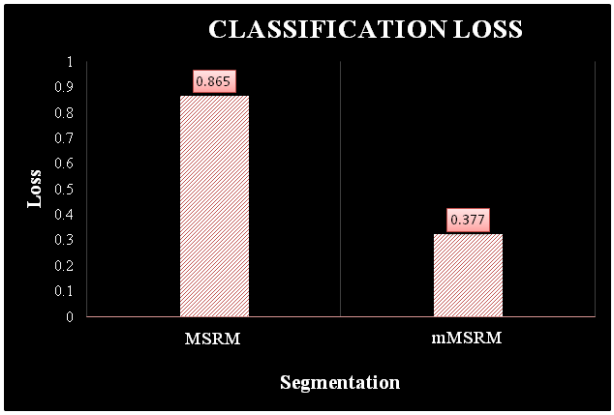

Fig. 4. Classification Loss Comparison

We got the accuracy of our work as 97 % and have reduced the classification loss to 0.321.

V. CONCLUSION

An Interactive Segmentation is more accurate as in human investigation and is faster as in automatic segmentation process. We proposed here in our paper, an interactive and a different approach of processing images with a view to find out the gliomas in multi-modal MR images. Skull stripping is the preprocessing method used for the removal of non – brain tissues. Later, the Interactive Segmentation (IS) and SVM classification is proposed in this work. For more accuracy, former probabilities are generated for the tumor and normal labels. The ASA process is implemented to select the adjacent tissue with respect to the intensity of the channel and label posteriors. The Gaussian Inception (GI) is employed to extract the features from the input MR images with reduced loss. Some of the features like mean, entropy, energy, standard deviation are extracted for the classification. The number of input samples is classifier under SVM classifier. The accuracy of our work is greatly improved in contrast with the existing work in brain MRI.

REFERENCES

1. Menze, B.H., Jakab, A., Bauer, S., Kalpathy-Cramer, J., Farahani, K., Kirby, J., Burren, Y., Porz, N., Slotboom, J., Wiest, R. and Lanczi, L., "The multimodal brain tumor image segmentation benchmark (BRATS)," IEEE transactions on medical imaging, 34(10), 2015, pp.1993-2024.
2. Fujiwara, N., Sakatani, K., Katayama, Y., Murata, Y., Hoshino, T., Fukaya, C. and Yamamoto, T., "Evoked-cerebral blood oxygenation changes in false-negative activations in BOLD contrast functional MRI of patients with brain tumors," Neuroimage, 21(4), 2004, pp.1464-1471.
3. Irimia, A., Chambers, M.C., Alger, J.R., Filippou, M., Prastawa, M.W., Wang, B., Hovda, D.A., Gerig, G., Toga, A.W., Kikinis, R. and Vespa, P.M., "Comparison of acute and chronic traumatic brain injury using semi-automatic multimodal segmentation of MR volumes," Journal of Neurotrauma, 28(11), 2011, pp.2287-2306.
4. Shenton, M.E., Hamoda, H.M., Schneiderman, J.S., Bouix, S., Pasternak, O., Rathi, Y., Vu, M.A., Purohit, M.P., Helmer, K., Koerte, I. and Lin, A.P., "A review of magnetic resonance imaging and diffusion tensor imaging findings in mild traumatic brain injury," Brain imaging and behavior, 6(2), 2012, pp.137-192.
5. Farr, T.D. and Wegener, S., "Use of magnetic resonance imaging to predict outcome after stroke: a review of experimental and clinical evidence," Journal of Cerebral Blood Flow & Metabolism, 30(4), 2010, pp.703-717.

6. Rekik, I., Allassonnière, S., Carpenter, T.K. and Wardlaw, J.M, "Medical image analysis methods in MR/CT-imaged acute-subacute ischemic stroke lesion: Segmentation, prediction and insights into dynamic evolution simulation models. A critical appraisal," NeuroImage: Clinical, 1(1), 2012, pp.164-178.
7. Phillips, W.E., Velthuizen, R.P., Phuphanich, S., Hall, L.O., Clarke, L.P. and Silbiger, M.L., "Application of fuzzy c-means segmentation technique for tissue differentiation in MR images of a hemorrhagic glioblastoma multiform," Magnetic resonance imaging, 13(2), 1995, pp.277-290.
8. Clark, M.C., Hall, L.O., Goldgof, D.B., Velthuizen, R., Murtagh, F.R. and Silbiger, M.S., "Automatic tumor segmentation using knowledge-based techniques," IEEE transactions on medical imaging, 17(2), 1998, pp.187-201.
9. Fletcher-Heath, L.M., Hall, L.O., Goldgof, D.B. and Murtagh, F.R., "Automatic segmentation of non-enhancing brain tumors in magnetic resonance images," Artificial intelligence in medicine, 21(1), 2001, pp.43-63.
10. Lee, C.H., Wang, S., Murtha, A., Brown, M.R. and Greiner, R., "Segmenting brain tumors using pseudo–conditional random fields. In International Conference on Medical Image Computing and Computer-Assisted Intervention," Springer, 2008, pp. 359-366.
11. Prastawa, M., Bullitt, E., Ho, S. and Gerig, G., "A brain tumor segmentation framework based on outlier detection," Medical image analysis, 8(3), 2004, pp.275-283.
12. Wels, M., Carneiro, G., Aplas, A., Huber, M., Hornegger, J. and Comaniciu, D., "A discriminative model-constrained graph cuts approach to fully automated pediatric brain tumor segmentation in 3-D MRI," Medical Image Computing and Computer-Assisted Intervention–MICCAI, 2008, pp.67-75.
13. Tu, Z., "Probabilistic boosting-tree: Learning discriminative models for classification, recognition, and clustering," Computer Vision, Tenth IEEE International Conference, Vol. 2, 2005, pp. 1589-1596.
14. Prastawa, M., Bullitt, E., Moon, N., Van Leemput, K. and Gerig, G., "Automatic brain tumor segmentation by subject specific modification of atlas priors," Academic radiology, 10(12), 2003, pp.1341-1348.
15. Y.-L. You, W. Xu, A. Tannenbaum, and M. Kaveh, "Behavioral analysis of anisotropic diffusion in image processing," IEEE Transactions on Image Processing, vol. 5, no. 11, 1996, pp. 1539-1553.
16. J. Weickert, "Anisotropic Diffusion in Image Processing," Teubner Stuttgart, vol. 1, 1998.
17. T. Ogden, "Essential Wavelets for Statistical Applications and Data Analysis," Springer, 1997.
18. R. D. Nowak, "Wavelet-based rician noise removal for magnetic resonance imaging," IEEE Transactions on Image Processing, vol. 8, no. 10, 1999, pp. 1408-1419.
19. A. Buades, B. Coll, and J.-M. Morel, "A non-local algorithm for image denoising, in Computer Vision and Pattern Recognition," IEEE Computer Society Conference, vol. 2, 2005, pp. 60-65.
20. J. V. Manj ´on, P. Coup´e, L. Mart´ı-Bonmat´ı, D. L. Collins, and M. Robles, "Adaptive non-local means denoising of mr images with spatially varying noise levels," Journal of Magnetic Resonance Imaging, vol. 31, no. 1, 2010, pp. 192-203.
21. S. Prima and O. Commowick, "Using bilateral symmetry to improve non-local means denoising of mr brain images in Biomedical Imaging," IEEE 10th International Symposium, IEEE, 2013, pp. 1231-1234.
22. P. Hoyer, "Independent component analysis in image denoising," Master degree dissertation, Helsinki University of Technology, 1999.
23. K. Phatak, S. Jakhade, A. Nene, R. Kamathe, and K. Joshi, "De-noising of magnetic resonance images using independent component analysis," Recent Advances in Intelligent Computational Systems (RAICS), 2011, pp. 807-812.
24. I. Diaz, P. Boulanger, R. Greiner, and A. Murtha, "A critical review of the effects of de-noising algorithms on mri brain tumor segmentation," Engineering in Medicine and Biology Society, EMBC, 2011, pp. 3934-3937.
25. C. Fennema-Notestine, I. B. Ozyurt, C. P. Clark, S. Morris, A. Bischoff-Grethe, M. W. Bondi, T. L. Jernigan, B. Fischl, F. Segonne, D. W. Shattuck, et al., "Quantitative evaluation of automated skull-stripping methods applied to contemporary and legacy images: Effects of diagnosis, bias correction, and slice location," Human Brain Mapping, vol. 27, no. 2, 2006, pp. 99-113.
26. A. H. Zhuang, D. J. Valentino, and A. W. Toga, "Skull stripping magnetic resonance brain images using a model based level set," NeuroImage, vol. 32, no. 1, 2006, pp. 79-92.
27. R. Roslan, N. Jamil, and R. Mahmud, "Skull stripping magnetic resonance images brain images: Region growing versus mathematical morphology," International Journal of Computer Information Systems and Industrial Management Applications, vol. 3, 2011, pp. 150-158.
28. S. Bauer, L.-P. Nolte, and M. Reyes, "Skull-stripping for tumor-bearing brain images," arXiv preprint arXiv: 1204.0357, 2012.
29. S. F. Eskildsen, P. Coup ´e, V. Fonov, J. V. Manj ´on, K. K. Leung, N. Guizard, S. N. Wassef, L. R. Østergaard, and D. L. Collins, "Beast: Brain extraction based on nonlocal segmentation technique," NeuroImage, vol. 59, no. 3, 2012, pp. 2362-2373.
30. F. S ´egonne, A. Dale, E. Busa, M. Glessner, D. Salat, H. Hahn, and B. Fischl, "A hybrid approach to the skull stripping problem in mri," Neuroimage, vol. 22, no. 3, 2004, pp. 1060-1075.
31. N. F. Ishak, R. Logeswaran, and W.-H. Tan, "Artifact and noise stripping on low-field brain mri," Int. J. Biology Biomed. Eng, vol. 2, no. 2, 2008, pp. 59-68.
32. S. Shen, W. Sandham, M. Granat, and A. Sterr, "Mri fuzzy segmentation of brain tissue using neighborhood attraction with neural-network optimization," IEEE Transactions on Information Technology in Biomedicine, vol. 9, no. 3, 2005, pp. 459-467.
33. J. G. Park and C. Lee, "Skull stripping based on region growing for magnetic resonance brain images," Neuro Image, vol. 47, no. 4, 2009, pp. 1394-1407.
34. W. Speier, J. E. Iglesias, L. El-Kara, Z. Tu, and C. Arnold, "Robust skull stripping of clinical glioblastoma multi forme data," Medical Image Computing and Computer-Assisted Intervention-MICCAI, Springer, 2011, pp. 659-666.
35. L. G. Nyu and J. K. Udupa, "Standardizing the MR image intensity scale," Image, vol. 1081, 1999.
36. A. Ekin, "Pathology-robust mr intensity normalization with global and local constraints," Biomedical Imaging: from Nano to Macro, 2011, pp. 333-336.
37. M. Shah, Y. Xiao, N. Subbanna, S. Francis, D. L. Arnold, D. L. Collins, and T. Arbel, "Evaluating intensity normalization on mris of human brain with multiple sclerosis," Medical Image Analysis, vol. 15, no. 2, 2011, pp. 267-282.
38. A. Mang, J. A. Schnabel, W. R. Crum, M. Modat, O. Camara-Rey, C. Palm, G. B. Caseiras, H. R. J¨ ager, S. Ourselin, T. M. Buzug, et al., "Consistency of parametric registration in serial mri studies of brain tumor progression," International Journal of Computer Assisted Radiology and Surgery, vol. 3, nos. 3-4, 2008, pp. 201-211.
39. X. Ren, J. Malik, "Learning a classification model for segmentation," ICCV03, vol.1, 2003, pp. 10–17.
40. Y. Cheng, "Mean shift, mode seeking, and clustering," IEEE Transactions on Pattern Analysis and Machine Intelligence, 17 (8), 1995, pp. 790–799.
41. D. Comaniciu, P. Meer, "Mean shift: a robust approach toward feature space analysis," IEEE Transactions on Pattern Analysis and Machine Intelligence, 24 (5), 2002, pp. 603–619.
42. L. Vincent, P. Soille, "Watersheds in digital spaces: an efficient algorithm based on immersion simulations," IEEE Transactions on Pattern Analysis and Machine Intelligence, 13 (6), 1991, pp. 583–598.
43. B. Sumengen, "Variational image segmentation and curve evolution on natural images," Ph.D. Thesis, University of California.
44. S. Birchfield, "Elliptical head tracking using intensity gradients and color histograms," Proceedings of IEEE Conference on Computer Vision and Pattern Recognition, 1998, pp. 232–237.
45. T. Ojala, M. Pietik¨ ainen, T. M¨ aenp¨ a¨ a, "Multiresolution gray-scale and rotation invariant texture classification with local binary patterns," IEEE Transactions on Pattern Analysis and Machine Intelligence, 24 (7), 2002, pp. 971–987.
46. M.J. Swain, D.H. Ballard, "Color indexing," International Journal of Computer Vision, 7 (1), 2002, pp. 11–32.
47. D. Comaniciu, V. Ramesh, P. Meer, "Kernel-based object tracking," IEEE Transactions on Pattern Analysis and Machine Intelligence, 25 (5), 2003, pp. 564–577.
48. K. Fukunaga, "Introduction to Statistical Pattern Recognition," second ed., Academic Press, 1990.
49. P. Felzenszwalb, D. Huttenlocher, "Efficient graph-based image segmentation," International Journal of Computer Vision, 59 (2), 2004, pp. 167–181.
50. Q. Yang, C. Wang, X. Tang, M. Chen, Z. Ye, "Progressive cut: an image cutout algorithm that models user intentions," IEEE Multimedia, 14 (3), 2007, pp. 56–66.
51. Y. Li, J. Sun, C. Tang, H. Shum, "Lazy snapping," SIGGRAPH 23, 2004, pp. 303–308.

52. Zhang, J., Ma, K.K., Er, M.H. and Chong, V., "Tumor segmentation from magnetic resonance imaging by learning via one-class support vector machine," International Workshop on Advanced Image Technology, 2004, pp. 207-211.
53. Garima Singh Rawat, Joy Bhattacharjee, Roopali Soni, "Proposed Method for Image Segmentation Using Similarity Based Region Merging Techniques," International Journal of Computer Science and Information Technologies, 3(5), 2012, pp. 5128 – 5132.
54. Agus Zainal Arifin, Rarasmaya Indraswari, Nanik Suciati, Eha Renwi Astuti and Dini Adni Navastara, "Region Merging Strategy Using Statistical Analysis for Interactive Image Segmentation on Dental Panoramic Radiographs," International Review on Computers and Software,12(1), 2017, pp. 63-74.

AUTHORS PROFILE

Dr. B. Perumal was born at Bodinayakanur, Tamilnadu, India, in the year 1980. He was graduated from his under graduation course in the department of Electronics and Communication Engineering from Madurai Kamaraj University, Madurai and was post graduated in the department of Digital Communication and Network Engineering in the year 2006 from Anna University, Chennai, India. He has done his Doctoral Programme on the concept of Medical Image Compression under Medical Image Processing in the year 2016 from Kalasalingam Academy of Research and Education, Krishnankoil, Srivilliputhur. He has done his Post Doctoral Fellowship in the year 2018 from Cracow University of Technology, Poland. Now he is currently working as Associate Professor in the Department of Electronics and Communication Engineering, Kalasalingam Academy of Research and Education, Srivilliputhur. He has so far published in more than 10 International Journals and presented about 19 papers in International Level Conferences and about 15 papers in National level Conferences. He has also attended many national and international level seminars and workshops. He is a fellow of Institute of Electrical and Electronics Engineers (IEEE). His research interests include Mobile Computing, Computer Vision, Wireless Sensor Networks, Cloud computing, and Bio-medical Instrumentation, Medical Image Compression in Medical Image Processing.

R.Sindhiya Devi,* was born in a small village town Surandai, Tirunelveli District of Tamilnadu, India in the year 1988. She completed her under graduation in the department of Electronics and Communication Engineering in the year 2010 from Einstein College of Engineering, Seethaparpanallur, Tirunelveli. Also, she completed her post graduation in the stream of Applied Electronics in the year 2014 from Einstein College of Engineering, Seethaparpanallur, Tirunelveli. She has also completed Master of Business Administration in Human Resource Management through Tamilnadu Open University, Tamilnadu. She is currently doing her Doctoral Programme on Medical Image Processing under the brain tumour detection from the department of Electronics and Communication Engineering as a part time Research Scholar in Kalasalingam Academy of Research and Education, Krishnankoil, Srivilliputhur. She started her career as a Lecturer in M.S.P.V.L Polytechnic College, Pavoorchatram. Then, she worked as a Guest Lecturer in Kamarajar Government Arts College, Surandai and continued her career as an Assistant Professor in Einstein College of Engineering, Tirunelveli. She has attended many national and international level seminars and workshops. She has also presented papers in International Level Conferences related to image processing. She is a member of Institute of Electrical and Electronics Engineers (IEEE). Her research interests include Computer Vision, Bio-medical Instrumentation and Medical Image Processing.

Pallikonda Rajasekaran Murugan Born in Srivilliputhur, Virudhunagar District of Tamil Nadu in 1980, he had his schooling in the same town and graduated in Electronics and Instrumentation Engineering in 2001 from Shanmugha College of Engineering, Thanjavurand completed his M.Tech. degree in 2002 with second Rank in SASTRA University. He pursued his doctoral programme in Anna University, Chennai. Starting as a Lecturer in 2003, he became Asst. Professor in 2008, Associate Professor in 2009 and Professor in 2012 in Kalasalingam Academy of Research and Education. He had a deep involvement in Bio-signal Processing research. His work is on the Image Segmentation for identification of brain tumour and image reconstruction and compression using medical images for diagnosis. Over 150 B.Tech students, 75 M.Tech students, and 8 Doctorates stand testimony for his productivity in Image Processing, Wireless Sensor Networks, and Biomedical Instrumentation research. He has so far published more than 50 papers in national and international journals and conferences. He is a Fellow of Indian Society For Technical Education (ISTE), Institute of Electrical and Electronics Engineers (IEEE), Asia-Pacific Chemical, Biological& Environmental Engineering Society (APCBEES), Institution of Engineers (India)(IE), International Association of Engineers (IAENG) and International Association of Computer Science and Information Technology (IACSIT).